DALTON
FULL PAPER

Synthesis of η^6-arene complexes of molybdenum containing β-ketophosphine and related P,O mixed donor ligands

Neale G. Jones,[a] Malcolm L. H. Green,*[a] Ino C. Vei,[a] Leigh H. Rees,[a] Sofia I. Pascu,[a] David Watkin,[a] Andrew Cowley,[a] Xavier Morise*[b] and Pierre Braunstein*[b]

[a] *Inorganic Chemistry Laboratory, University of Oxford, South Parks Road, Oxford, UK OX1 3QR. E-mail: Malcolm.Green@chemistry.oxford.ac.uk.*
[b] *Université Louis Pasteur, Laboratoire de Chimie de Coordination (UMR 7513 CNRS), 4 rue Blaise Pascal, F-67070 Strasbourg, France. E-mail: morise@chimie.u-strasbg.fr; braunst@chimie.u-strasbg.fr.*

Received 8th March 2002, Accepted 26th March 2002
First published as an Advance Article on the web 15th May 2002

The reactions of the ligands $Ph_2PCH_2C(O)R$ (R = Ph, NPh_2) with the η^6-arene molybdenum complexes $[Mo(\eta^3\text{-}C_3H_5)(\mu\text{-}Cl)(\eta^6\text{-}C_6H_5R)]_2$ (R = H, Me) have been investigated. A series of complexes in which the keto- or amidophosphine acts as a monodentate P ligand or as a neutral or anionic P,O chelating ligand have been synthesised and characterised. The crystal structures of the compounds $[Mo(\eta^3\text{-}C_3H_5)Cl(\eta^6\text{-}C_6H_5Me)\{Ph_2PCH_2C(O)Ph\}]$, $[Mo(\eta^3\text{-}C_3H_5)\{Ph_2PCH_2C(O)NPh_2\text{-}\kappa^2P,O\}(\eta^6\text{-}C_6H_5Me)][PF_6]$ and $[Mo\{Ph_2PCH\cdots C(\cdots O)Ph\text{-}\kappa^2P,O\}_2(\eta^6\text{-}C_6H_5R)]$ (R = H, Me) have been determined. Interesting differences in the reactivity of the ketophosphine ligand *versus* the amidophosphine ligand were discovered and an unprecedented hydrogen–deuterium exchange of methylene and olefinic protons has been observed for the coordinated neutral or anionic ketophosphine ligands.

Introduction

Heterodifunctional ligands, such as the acetophenone derived β-ketophosphine $Ph_2PCH_2C(O)Ph$, represent an interesting class of ligands and their transition metal complexes have found many applications in stoichiometric and catalytic transformations of both academic and industrial relevance. However, to date, studies involving the β-ketophosphine ligands have mostly focused on the late transition metals (Groups 8 to 10).[1–7]

Furthermore, it is well established that the methylene protons of β-ketophosphine ligands are acidic and can be readily deprotonated to give the corresponding phosphinoenolate. Late transition metal complexes of the enolate form of this class of ligand have also been shown to be highly active catalysts for a range of reactions.[8–10] For example, anionic P,O ligands of this type have been shown to play a key role in the nickel-catalysed ethene oligomerization into linear α-olefins (Shell Higher Olefin Process).[11–14]

The early and middle transition metal chemistry of heterodifunctional phosphine ligands containing a carbonyl group, such as a ketone, ester or amide function, has not been extensively investigated. Half-sandwich molybdenum complexes of the amidophosphine $Ph_2PCH_2C(O)NPh_2$[15] and the keto-functionalised *N*-pyrrolylphosphine $Ph_2PNC_4H_3\{C(O)Me\}\text{-}2$[16] have been recently reported.

In the 1970s, it was observed that the $Mo(\eta^3\text{-allyl})(\eta^6\text{-arene})$ fragment exhibited some interesting reactivity with neutral and anionic chelating ligands possessing a variety of different donor atoms—P, N, S and O.[17–19]

Here we describe the chemistry of the β-keto and amidophosphine ligands $Ph_2PCH_2C(O)R$ (R = Ph, NPh_2), and related systems, with η^6-arene molybdenum(II) complexes.

Results and discussion

Reaction of $[Mo(\eta^3\text{-}C_3H_5)(\mu\text{-}Cl)(\eta^6\text{-}C_6H_5R)]_2$ (R = H, Me) with $Ph_2PCH_2C(O)Ph$

The reaction between $[Mo(\eta^3\text{-}C_3H_5)(\mu\text{-}Cl)(\eta^6\text{-}C_6H_5R)]_2$ (R = H, Me) and (diphenylphosphino)acetophenone, $Ph_2PCH_2C(O)Ph$, in ethanol resulted in cleavage of the chloro-bridged dimer to afford the phosphine adduct $[Mo(\eta^3\text{-}C_3H_5)Cl(\eta^6\text{-}C_6H_5R)\text{-}\{Ph_2PCH_2C(O)Ph\}]$ [R = H (**1a**), Me (**1b**)] as a purple solid in 60–65% yield (Scheme 1). The characterising data for **1**, and all new compounds described in this paper (**2**–**7**), are listed in Table 1.

Since the complex is chiral at molybdenum, the methylene protons are diastereotopic and therefore magnetically inequivalent. The methylene protons were observed as an AB system in the ^1H NMR spectrum (Table 1). The IR spectrum confirmed that the carbonyl fragment of the ketophosphine ligand was not coordinated to the metal centre (ν_{CO} 1678 cm^{-1} for **1a** and 1674 cm^{-1} for **1b** *vs.* 1680 cm^{-1} for the free ligand[20]). The ^{31}P NMR spectra displayed resonances shifted approximately 57 ppm downfield of the free phosphine (δ −17.1 ppm).[20] This is consistent with coordination of the phosphorus to a molybdenum(II) metal centre.[15]

X-Ray quality crystals of **1b** were grown *via* the slow diffusion of pentane into a concentrated dichloromethane solution of the complex. The molecular structure of **1b** is shown in Fig. 1. Selected bond distances and angles are presented in Table 2.

The complex adopts a three-legged piano stool structure, with the Mo–allyl centroid vector taken as one of the legs of the stool. The average L–Mo–L angle of 90.6° and the average arene centroid–Mo–L angle of 123.9° are similar to those observed in other molybdenum three-legged piano stool structures.[21,22] The Mo–ligand bond lengths are within the expected ranges.[22–25]

The crystal structure confirms that the ketophosphine behaves as a monodentate phosphorus ligand. The methyl group of the coordinated toluene ligand and the molybdenum-bound chloride adopt an eclipsed conformation (Fig. 2). The C(44)–Cl(1) distance of 3.35 Å and the Mo(1)–Cl(1) ··· H angle of approximately 86° are consistent with a hydrogen-bonding type interaction.[26] This interaction holds the conformation of the η^6-arene ligand in the solid state. A further close

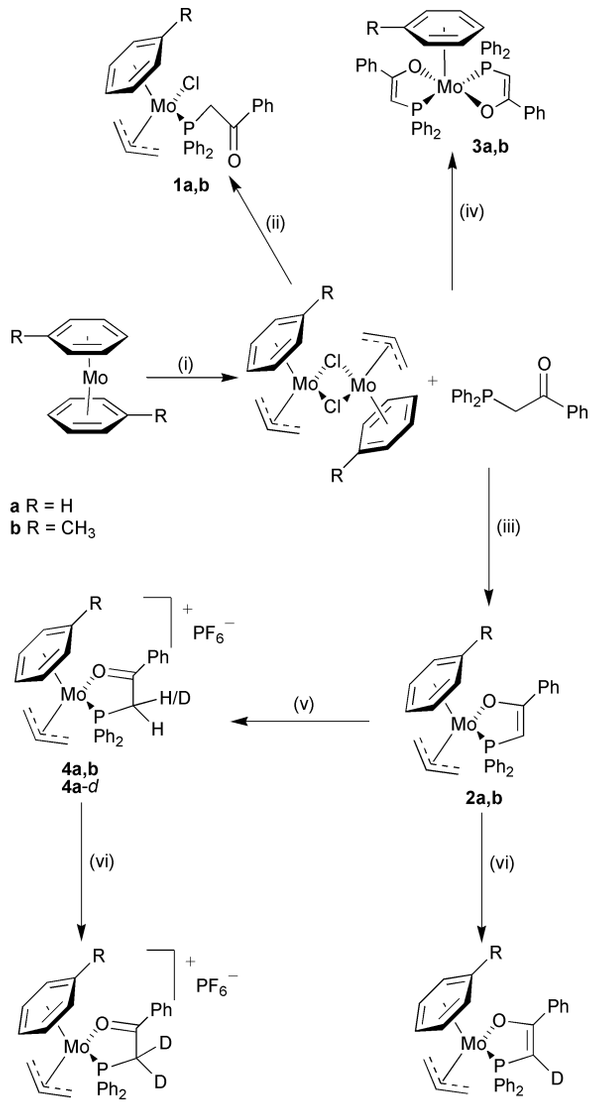

Scheme 1 *Reagents and conditions*: (i) C_3H_5Cl; (ii) ethanol; (iii) ethanol, NEt_3; (iv) ethanol, reflux; (v) pyridinium hexafluorophosphate, ethanol; for **4a**-*d*, pyridinium-*d* hexafluorophosphate; (vi) CD_2Cl_2, D_2O.

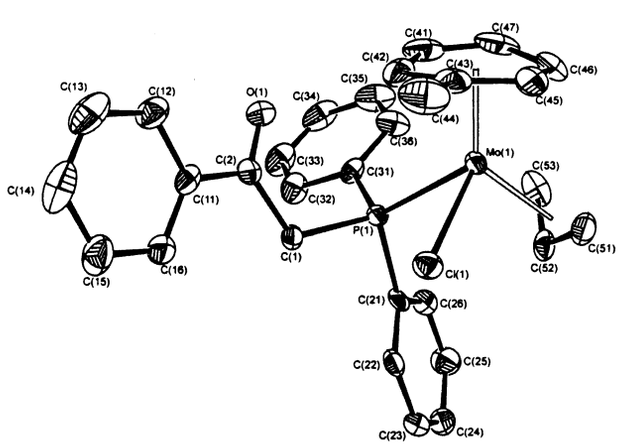

Fig. 1 The molecular structure of $[Mo(\eta^3\text{-}C_3H_5)Cl(\eta^6\text{-}C_6H_5Me)\{Ph_2PCH_2C(O)Ph\}]$, **1b** (50% thermal ellipsoids). Hydrogen atoms have been omitted for clarity.

contact is observed between the oxygen of the carbonyl ligand, O(1), and C(41) (3.07 Å) and C(42) (3.25 Å) of the η^6-toluene ligand. These separations equate to approximate O–H distances of 2.36 and 2.78 Å, respectively (Fig. 2).

Of more interest is the close contact between the molybdenum-bound chloride and the methylene group of the

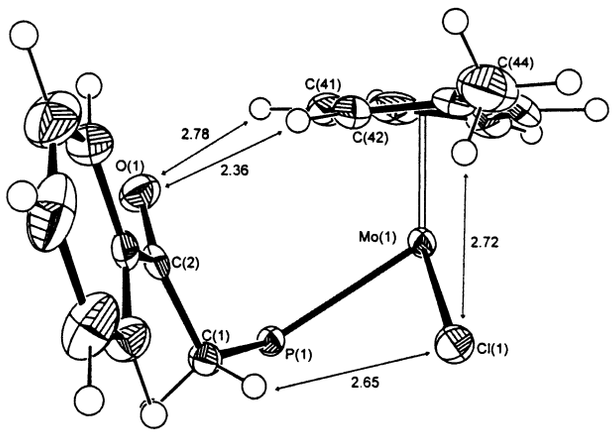

Fig. 2 Partial molecular structure of $[Mo(\eta^3\text{-}C_3H_5)Cl(\eta^6\text{-}C_6H_5Me)\{Ph_2PCH_2C(O)Ph\}]$, **1b** (50% thermal ellipsoids), showing close contacts and hydrogen-bonding interactions.

ketophosphine ligand (Fig. 2), with Cl(1)–C(1) = 3.301, Cl(1)–H = 2.65 Å and Mo(1)–Cl(1)–H = 92.5°. The observed structural features are strongly suggestive of a hydrogen-bonding interaction.[26]

The η^6-toluene ligand is distorted into a boat conformation, with 2 carbon atoms [C(42) and C(46)] pulled closer to the metal centre.[23,27,28] The fold angle of the arene along the C(42)–C(46) vector is 10.7°. This is consistent with the fold angles observed in other transition metal arene complexes.[28] There is also a distinct variation in the C–C bond lengths of the aromatic system, tending towards a 1,4-dienyl type structure, with Δ = (1.413–1.372) = 0.041.[29] Δ is defined as the difference between the average C–C single bond lengths and the average C–C double bond lengths, and was proposed as a quantitative measure of the π-electron localisation in the arene ring.

The reaction between $[Mo(\eta^3\text{-}C_3H_5)(\mu\text{-}Cl)(\eta^6\text{-}C_6H_5R)]_2$ (R = H, Me) and (diphenylphosphino)acetophenone, $Ph_2PCH_2C(O)Ph$, in the presence of excess triethylamine and ethanol as solvent yielded the η^2-phosphinoenolate complexes $[Mo(\eta^3\text{-}C_3H_5)\{Ph_2PCH\cdots C(\cdots O)Ph\text{-}\kappa^2P,O\}(\eta^6\text{-}C_6H_5R)]$ [R = H (**2a**), Me (**2b**)] as orange solids in 60–80% yield (Scheme 1). We note the mild conditions under which the ketophosphine ligand is deprotonated (with elimination of the chloro ligand) to yield the metallocyclic fragment. In general, complexes of this type are prepared either *via* deprotonation of the corresponding η^2-ketophosphine complex with a strong base, *e.g.* hydride bases,[4–6] alkoxide bases[9] or alkyl lithium reagents, or *via* reaction of the pre-formed alkali metal enolate with a complex containing a metal–halide bond.[30,31]

Interestingly, the reaction between $[Mo(\eta^3\text{-}C_3H_5)(\mu\text{-}Cl)(\eta^6\text{-}C_6H_5R)]_2$ (R = H, Me) and $Ph_2PCH_2C(O)Ph$ in refluxing ethanol yielded the bis-η^2-phosphinoenolate complexes $[Mo\{Ph_2PCH\cdots C(\cdots O)Ph\text{-}\kappa^2P,O\}_2(\eta^6\text{-}C_6H_5R)]$ [R = H (**3a**), Me (**3b**)] as dark red solids in 15–20% yield (Scheme 1).

Attempts to investigate the mechanism for the formation of the bis-phosphinoenolate complexes **3** did not yield any meaningful insights. Two possible mechanisms are presented in Scheme 2.

It is unclear whether the molybdenum–allyl bond is cleaved by direct reaction with a β-ketophosphine ligand or by reaction with HCl eliminated from a phosphine chloride complex.

X-Ray quality crystals of **3a** and **3b** were grown *via* the slow diffusion of pentane into a concentrated dichloromethane solution of the bis-phosphinoenolate complex. The crystal structures of the complexes **3a** and **3b** have been determined and the molecular structures are displayed in Fig. 3 and 5, respectively. Selected bond distances and angles are presented in Tables 3 (**3a**) and 4 (**3b**).

Both the bis-phosphinoenolate complexes **3** adopt a four-legged piano stool structure with the two phosphorus donor atoms lying *trans* to one another (Fig. 4).

Table 1 Analytical and spectroscopic data for **1**–**7**

Compound and analytical data [a]	NMR [b] and IR [c] data
1a [Mo(η^3-C_3H_5)Cl(η^6-C_6H_6){$Ph_2PCH_2C(O)Ph$}]; purple crystals; C 62.5 (62.8), H 5.5 (5.1)	^{1}H [d]: 7.23–7.92 (m, 15H, Ph), 5.15 (dd, J_{PH} = 5.1, J_{HH} = 17.0, 1H, CH_2), 4.68 (s, 6H, C_6H_6), 4.25 (dd, J_{PH} = 11.1, J_{HH} = 17.0, 1H, CH_2), 2.97 (m, 1H, allyl-H_c), 2.92 (m, 1H, allyl-H_t), 2.28 (m, 1H, allyl-H_t), 1.76 (m, 1H, allyl-H_t), 1.59 (m, 1H, allyl-H_t). ^{13}C-{^{1}H} [d]: 196.2 (d, J_{PC} = 3.4, CO), 137.9 (d, J_{PC} = 3, Ph), 135.2 (d, J_{PC} = 30.8, Ph_2P), 134.4 (d, J_{PC} = 34.1, Ph_2P), 133.9 (d, J_{PC} = 9.8, Ph_2P), 133.4 (s, Ph), 132.2 (d, J_{PC} = 7.3, Ph_2P), 130.1 (d, J_{PC} = 1.9, Ph_2P), 129.4 (d, J_{PC} = 2.6, Ph_2P), 128.7 (s, Ph), 128.6 (s, Ph), 128.2 (d, J_{PC} = 8.6, Ph_2P), 127.6 (d, J_{PC} = 8.5, Ph_2P), 97.1 (d, J_{PC} = 1.2, C_6H_6), 84.7 (d, J_{PC} = 1.4, allyl-C_c), 53.1 (d, J_{PC} = 2.3, allyl-C_t), 43.8 (d, J_{PC} = 7.5, allyl-C_t), 37.5 (d, J_{PC} = 21.6, PCH_2). ^{31}P-{^{1}H} [d]: 35.3 (s, CH_2PPh_2). IR: 1678 (s, ν_{CO}).
1b [Mo(η^3-C_3H_5)Cl(η^6-C_6H_5Me){$Ph_2PCH_2C(O)Ph$}]; purple crystals; C 62.9 (63.3), H 5.2 (5.3)	^{1}H [d] 7.26–7.90 (m, 15H, Ph), 5.05 (dd, J_{PH} = 5.1, J_{HH} = 16.8, 1H, CH_2), 5.06 (m, 1H, Tol), 4.68 (t, J_{HH} = 6.3, 1H, Tol), 4.57 (d, J_{HH} = 6.0, 1H, Tol), 4.33 (d, J_{HH} = 4.8, 1H, Tol), 4.26 (dd, J_{PH} = 10.4, J_{HH} = 16.7, 1H, CH_2), 4.06 (t, J_{HH} = 5.7, 1H, Tol), 2.97 (m, 1H, allyl), 2.61 (dd, J_{HH} = 8.7, J_{HH} = 3.0, 1H, allyl), 2.33 (dd, J_{HH} = 6.3, J_{HH} = 3.3, 1H, allyl), 1.74 (m, 1H, allyl), 1.66 (s, 3H, Tol-CH_3), 1.38 (t, J_{HH} = 7.2, 1H, allyl). ^{13}C-{^{1}H} [d]: 196.5 (s, CO), 138.2 (s, Ph), 134.1 (s, Ph), 134.0 (s, Ph), 133.4 (s, Ph), 132.5 (s, Ph), 132.4 (s, Ph), 130.2 (s, Ph), 129.5 (s, Ph), 128.3 (s, Ph), 128.2 (s, Ph), 127.8 (s, Ph), 127.7 (s, Ph), 100.1 (s, Tol), 97.2 (s, Tol), 95.6 (s, Tol), 94.3 (s, Tol), 93.9 (s, Tol), 93.7 (s, Tol), 84.1 (s, allyl), 44.0 (s, allyl), 37.5 (d, J_{PC} = 20.2, PCH_2), 19.1 (s, Tol-CH_3). ^{31}P-{^{1}H} [d]: 36.4 (s, CH_2PPh_2). IR: 1674 (s, ν_{CO}).
2a [Mo(η^3-C_3H_5){$Ph_2PCH{\cdots}C(\underline{\cdots}O)Ph$-$\kappa^2$*P,O*}-($\eta^6$-$C_6H_6$)]; orange crystals; C 66.8 (67.2), H 5.2 (5.3)	^{1}H [d]: 7.84 (m, 2H, Ph), 7.66 (m, 4H, Ph), 7.50–7.26 (m, 9H, Ph), 5.05 [d, J_{PH} = 1.2, 1H, PC*H*C(Ph)O], 4.53 (d, J_{PH} = 1.2. 6H, C_6H_6), 3.22 (m, 1H, allyl-H_c), 2.96 (dd, J_{HH} = 2.3, J_{HH} = 7.7, allyl-H_t), 1.96 (dd, J_{HH} = 2.6, J_{HH} = 5.8, allyl-H_t), 1.49 (m, 1H, allyl-H_t), 0.53 (t, J_{HH} = 6.6, 1H, allyl-H_t). ^{13}C-{^{1}H} [d]: 185.3 (d, J_{PC} = 24.9, C=*C*–O), 139.5 (s, Ph), 139.4 (d, J_{PC} = 41.9, Ph_2P), 134.9 (d, J_{PC} = 32.5, Ph_2P), 132.2 (d, J_{PC} = 9.5, Ph_2P), 131.5 (d, J_{PC} = 9.5, Ph_2P), 128.9 (d, J_{PC} = 2.1, Ph_2P), 128.6 (d, J_{PC} = 2.1, Ph_2P), 128.5 (s, Ph), 128.2 (d, J_{PC} = 8.9, Ph_2P), 127.8 (d, J_{PC} = 8.9, Ph_2P), 127.8 (s, Ph), 126.8 (s, Ph), 96.8 (d, J_{PC} = 1.1, C_6H_6), 78.0 (s, allyl-C_c), 75.4 (d, J_{PC} = 54.4, P*C*H=C), 50.0 (d, J_{PC} = 1.6, allyl-C_t), 40.2 (d, J_{PC} = 5.3, allyl-C_t). ^{31}P-{^{1}H} [d]: 56.4 (s, Ph_2PCH). IR: 1514 (m, $\nu_{C=C\ +\ C=O}$).
2b [Mo(η^3-C_3H_5){$Ph_2PCH{\cdots}C(\underline{\cdots}O)Ph$-$\kappa^2$*P,O*}-($\eta$-$C_6H_5Me$)]; orange crystals; C 67.0 (67.7), H 5.8 (5.5)	^{1}H [e]: 7.04–7.98 (m, 15H, Ph), 5.19 (d, J_{PH} = 1.5, 1H, PCH), 4.53 (m, 1H, Tol), 4.40 (m, 1H, Tol), 4.08 (m, 1H, Tol), 3.78 (m, 1H, allyl-H_c), 3.69 (m, 2H, Tol), 2.94 (dd, J_{HH} = 2.7, J_{HH} = 8.1, 1H, allyl-H_t), 2.58 (dd, J_{HH} = 3.3, J_{HH} = 6.0, 1H, allyl-H_t), 1.75 (m, 1H, allyl-H_t), 1.18 (s, 3H, Tol-CH_3), 0.55 (t, J_{HH} = 6.3, allyl-H_t). ^{13}C-{^{1}H} [d]: 184.5 (d, J_{PC} = 25.9, C=*C*–O), 139.6 (s, Ph), 139.4 (d, J_{PC} = 42.1, Ph_2P), 134.9 (d, J_{PC} = 34.8, Ph_2P), 132.2 (d, J_{PC} = 9.2, Ph_2P), 131.5 (d, J_{PC} = 9.2, Ph_2P), 128.8 (d, J_{PC} = 1.8, Ph_2P), 128.6 (d, J_{PC} = 2.1, Ph_2P), 128.4 (s, Ph), 128.1 (d, J_{PC} = 8.5, Ph_2P), 127.8 (d, J_{PC} = 8.0, Ph_2P), 127.8 (s, Ph), 126.8 (s, Ph), 101.8 (s, Tol), 96.8 (s, Tol), 95.7 (d, J_{PC} = 3.6, Tol), 95.5 (s, Tol), 90.3 (d, J_{PC} = 2.4, Tol), 88.1 (s, Tol), 76.9 (s, allyl-C_c), 75.3 (d, J_{PC} = 54.5, P*C*H=C), 50.1 (s, allyl-C_t), 40.0 (d, J_{PC} = 5.3, allyl-C_t), 19.1 (s, Tol-CH_3). ^{31}P-{^{1}H} [e]: 57.4 (s, $CHPPh_2$). IR: 1516 (m, $\nu_{C=C\ +\ C=O}$).
3a [Mo{$Ph_2PCH{\cdots}C(\underline{\cdots}O)Ph$-$\kappa^2$*P,O*}$_2$($\eta^6$-$C_6H_6$)]; purple crystals; C 70.4 (70.8), H 4.8 (4.9)	^{1}H [e]: 8.10–8.04 (m, 3H, Ph), 7.68–7.63 (m, 7H, Ph), 7.27–7.10 (m, 13H, Ph), 6.85–6.80 (m, 7H, Ph), 5.01 (t, J_{PH} = 0.9, 2H, PCHC), 3.88 (t, J_{PH} = 1.1, 6H, C_6H_6). ^{13}C-{^{1}H} [d]: 182.6 [d, J_{PC} = 28.5, =*C*(Ph)O], 143.8 (d, J_{PC} = 49.1, Ph), 139.9 (s, Ph), 138.7 (s, Ph), 131.8 (s, Ph), 130.2 (s, Ph), 128.0 (s, Ph), 127.7 (s, Ph), 127.5 (s, Ph), 127.4 (s, Ph), 127.1 (s, Ph), 125.9 (s, Ph), 98.0 (s, C_6H_6), 78.3 [d, J_{PC} = 54.0, Ph_2PC(H)=]. ^{31}P-{^{1}H} [e]: 51.8 (s, Ph_2PC). IR: 1522 (w, $\nu_{C=C\ +\ C=O}$).
3b [Mo{$Ph_2PCH{\cdots}C(\underline{\cdots}O)Ph$-$\kappa^2$*P,O*}$_2$($\eta^6$-$C_6H_5Me$)]; purple crystals; C 70.6 (71.0), H 5.1 (5.1)	^{1}H [e]: 6.83–8.14 (m, 30H, Ph), 5.54 (s, 2H, PCH=), 4.35–4.41 (m, 2H, Tol-H_{ortho} = H_{meta}), 4.17 (t, J_{HH} = 5.1, 1H, Tol-H_{meta}), 3.99 (d, J_{HH} = 5.4, 1H, Tol-H_{ortho}), 3.24 (t, J_{HH} = 6.2, 1H, Tol-H_{para}), 0.81 (s, 3H, Tol-CH_3). ^{31}P-{^{1}H} [e]; 54.1 (s, Ph_2PCH=). IR: 1522 (w, $\nu_{C=C\ +\ C=O}$).
4a [Mo(η^3-C_3H_5){$Ph_2PCH_2C(O)Ph$-κ^2*P,O*}(η^6-C_6H_6)][PF_6]; purple crystals; C 51.9 (52.4), H 4.3 (4.3)	^{1}H [d]: 8.05 (m, 2H, Ph), 7.79 (m, 1H, Ph), 7.61 (m, 7H, Ph), 7.42 (m, 3H, Ph), 7.02 (m, 2H, Ph), 4.94 (d, J_{PH} = 1.0, 6H, C_6H_6), 4.73 (dd, J_{PH} = 10.5, J_{HH} = 17.8, 1H, PCH_2), 4.14 (dd, J_{PH} = 8.4, J_{HH} = 17.8, 1H, PCH_2), 3.43 (dd, J_{HH} = 2.1, J_{HH} = 8.3, 1H, allyl-H_t), 3.27 (m, 1H, allyl-H_c), 2.48 (dd, J_{HH} = 2.8, J_{HH} = 6.2,1H, allyl-H_t), 2.16 (m, 1H, allyl-H_t), 1.61 (m, 1H, allyl-H_t). ^{13}C-{^{1}H} [d]: 212.2 (d, J_{PC} = 9.5, CO), 137.1 (s, Ph), 133.0 (s, Ph), 132.0 (s, Ph), 131.8 (s, Ph), 131.7 (s, Ph), 131.2 (s, Ph), 131.1 (s, Ph), 130.9 (s, Ph), 129.9 (s, Ph), 129.7 (s, Ph), 129.4 (s, Ph), 129.3 (s, Ph), 97.9 (s, C_6H_6), 82.5 (s, allyl-C_c), 48.7 (s, allyl-C_t), 43.6 (d, J_{PC} = 5, PCH_2), 43.1 (s, allyl-C_t). ^{31}P-{^{1}H} [d]: 69.3 (s, Ph_2PCH_2), −143.4 (sept, J_{PF} = 715, PF_6). IR: 1558 (s, ν_{CO}).

Table 1 (*Contd.*)

Compound and analytical data [a]	NMR [b] and IR [c] data
4b [Mo(η^3-C_3H_5){$Ph_2PCH_2C(O)Ph$-κ^2P,O}-(η^6-C_6H_5Me)][PF_6]; purple crystals; C 48.2 (48.7), H 4.3 (4.2) [1 equiv CH_2Cl_2]	^{1}H [d]: 8.06–8.03 (m, 2H, Ph), 7.81–7.78 (m, 1H, Ph), 7.65–7.39 (m, 10H, Ph), 7.08–7.03 (m, 2H, Ph), 5.14 (m, 1H, Tol), 4.95 (m, 1H, Tol), 4.86 (m, 1H, Tol), 4.69–4.63 (m, 2H, Tol, PCH_2), 4.55–4.53 (m, 1H, Tol), 4.17 (dd, J_{PH} = 8.4, J_{HH} = 18.0, 1H, PCH_2), 3.29 (m, 1H, allyl-H_c), 3.18 (dd, J = 2.1, J = 8.7, allyl-H_t), 2.48 (dd, J = 2.4, J = 6.0, allyl-H_t), 2.12 (m, 1H, allyl-H_t), 1.62 (s, 3H, Tol-CH_3), 1.42 (m, 1H, allyl-H_t). ^{31}P-{^{1}H} [d]: 69.3 (s, Ph_2PCH_2), −143.4 (sept, J_{PF} = 713, PF_6^-). IR: 1560 (s, ν_{CO}).
5 [Mo(η^3-C_3H_5)Cl(η^6-C_6H_5Me){$Ph_2PCH_2C(O)NPh_2$}]; purple–red solid; C 65.8 (65.5), H 5.4 (5.3), N 2.2 (2.1)	^{1}H [d]: 7.52–7.13 (m, 18H, Ph), 6.88 (br s, 2H, Ph), 5.16 (m, 1H, Tol), 4.68 (m, 2H, Tol), 4.36 (m, 1H, Tol), 4.12 (dd, J_{PH} = 5.8, J_{HH} = 15.7, 1H, PCH_2), 4.06 (m, 1H, Tol), 3.63 (dd, J_{PH} = 11.1, J = 15.7, 1H, PCH_2), 2.63 (m, 1H, allyl-H_c), 2.61 (m, 1H, allyl-H_t), 2.22 (m, 1H, allyl-H_t), 1.72 (s, 3H, Tol-CH_3), 1.67 (m, 1H, allyl-H_t), 1.31 (m, 1H, allyl-H_t). ^{13}C-{^{1}H} [d]: 167.7 (d, J = 3, C=O), 142.5 (s, Ph), 134.7 (d, J = 19, PPh), 134.3 (d, J = 19, PPh), 133.8 (d, J = 10, PPh), 131.9 (d, J = 8, PPh), 129.7 (d, J = 2, PPh), 129.5 (br, Ph), 128.7 (d, J = 2, PPh), 128.3 (br, Ph), 127.5 (d, J = 8, PPh), 126.7 (d, J = 8, PPh), 126.3 (br, Ph), 115.3 (d, J = 2.6, Tol), 99.3 (s, Tol), 96.7 (s, Tol), 95.3 (s, Tol), 93.8 (d, J = 2.8, Tol), 93.3 (d, J = 4.5, Tol), 83.9 (s, allyl-C_c), 53.6 (d, J = 2.2, allyl-C_t), 42.8 (d, J = 7.3, allyl-C_t), 35.6 (d, J = 22, PCH_2), 18.5 (s, Tol-CH_3). ^{31}P-{^{1}H} [d]: 40.0 (s, Ph_2PCH_2). IR: 1668 (s, ν_{CO}).
6 [Mo(η^3-C_3H_5){$Ph_2PCH_2C(O)NPh_2$-κ^2P,O}-(η^6-C_6H_5Me)][PF_6]; purple–red crystals; C 55.9 (56.2), H 4.7 (4.6), N 1.8 (1.8)	^{1}H [d]: 7.60–7.14 (m, 20H, Ph), 5.13 (m, 1H, Tol), 4.86 (m, 1H, Tol), 4.68 (m, 1H, Tol), 4.62 (m, 1H, Tol), 4.39 (m, 1H, Tol), 3.59 (m, 2H, PCH_2), 3.37 (m, 1H, allyl-H_c), 3.00 (dd, J = 2.6, J = 8.1, allyl-H_t), 2.09 (dd, J = 3, J = 6, allyl-H_t), 1.97 (m, 1H, allyl-H_t), 1.49 (s, 3H, Tol-CH_3), 1.11 (m, 1H, allyl-H_t). ^{13}C-{^{1}H} [d]: 178.5 (d, J = 16, C=O), 141.5 (s, Ph), 140.1 (s, Ph), 131.2 (d, J = 2.1, Ph), 131.1 (d, J = 1.8, Ph), 131.0 (s, Ph), 130.5 (br, Ph), 130.4 (s br, Ph), 130.3 (s, Ph), 129.3 (s br, Ph), 129.3 (s, Ph), 129.0 (d, J = 10.1, Ph), 128.7 (d, J = 9.9, Ph), 128.1 (s, Ph), 126.8 (s, Ph), 125.8 (s, Ph), 116.0 (s, Tol), 100.5 (s, Tol), 97.6 (s, Tol), 95.5 (s, Tol), 95.0 (d, J = 2.1, Tol), 94.8 (d, J = 9.7, Tol), 80.5 (s, allyl-C_c), 49.2 (s, allyl-C_t), 42.4 (d, J = 5.3, allyl-C_t), 39.0 (d, J = 26.1, PCH_2), 18.4 (s, Tol-CH_3). ^{31}P-{^{1}H} [d]: 61.9 (s, Ph_2PCH_2), −143.2 (sept, J_{PF} = 712, PF_6^-). IR: 1554 (s, ν_{CO}).
7 [Mo(η^3-C_3H_5){$Ph_2PCH\cdots C(\cdots O)NPh_2$-$\kappa^2P,O$}($\eta^6$-$C_6H_5Me$)]; orange solid; C 69.0 (69.3), H 5.6 (5.5), N 2.1 (2.3)	^{1}H [e]: 7.79–7.66 (m, 4H, Ph), 7.30–7.27 (m, 4H, Ph), 7.19–7.04 (m, 10H, Ph), 6.90–6.85 (m, 2H, Ph), 4.39 (m, 1H, Tol), 4.21 (m, 1H, Tol), 4.13 (m, 1H, Tol), 3.92 (m, 1H, allyl-H_c), 3.75 (d, J_{PH} = 1.6, PCHC), 3.62 (m, 2H, Tol), 2.74 (dd, J = 2.3, J = 8.1, 1H, allyl-H_t), 2.50 (dd, J = 3.4, J = 6.1, 1H, allyl-H_t), 1.78 (m, 1H, allyl-H_t), 1.18 (s, 3H, Tol-CH_3), 0.55 (t, J = 6.7, 1H, allyl-H_t). ^{31}P-{^{1}H} [e]: 48.6 (s, Ph_2PCH). IR: 1502 (s, $\nu_{C=C\ +\ C=O}$).

[a] Reported as percentages. Calculated values in parentheses. [b] NMR data are given as chemical shift (δ) (multiplicity, relative intensity, J/Hz, assignment). H/C_t = terminal, H/C_c = central. [c] Nujol mull. [d] Recorded in CD_2Cl_2. [e] Recorded in C_6D_6.

Table 2 Selected bond lengths (Å) and angles (°) for **1b**

Mo(1)–C(51)	2.254(3)	Mo(1)–C(41)	2.318(3)
Mo(1)–C(52)	2.186(3)	Mo(1)–C(42)	2.278(3)
Mo(1)–C(53)	2.254(3)	Mo(1)–C(43)	2.396(3)
Mo(1)–$Cent_{(allyl)}$	1.976	Mo(1)–C(45)	2.315(3)
Mo(1)–$C_{(average)}$	2.23	Mo(1)–C(46)	2.213(3)
		Mo(1)–C(47)	2.338(3)
Mo(1)–P(1)	2.5344(6)	Mo(1)–$Cent_{(Tol)}$	1.839
Mo(1)–Cl(1)	2.5070(6)	Mo(1)–$C_{(average)}$	2.31
$Cent_{(Tol)}$–Mo(1)–$Cent_{(allyl)}$	130.57	$Cent_{(allyl)}$–Mo(1)–Cl(1)	96.94
$Cent_{(Tol)}$–Mo(1)–Cl(1)	117.96	$Cent_{(allyl)}$–Mo(1)–P(1)	95.14
$Cent_{(Tol)}$–Mo(1)–P(1)	123.19	Cl(1)–Mo(1)–P(1)	79.69(2)
		O(1)–C(2)–C(1)	121.4(2)

Table 3 Selected bond lengths (Å) and angles (°) for **3a**

Mo(1)–P(1)	2.4421(3)	Mo(1)–C(21)	2.3645(14)
Mo(1)–O(1)	2.1140(9)	Mo(1)–C(22)	2.2825(14)
Mo(1)–$Cent_{(Tol)}$	1.825	Mo(1)–C(23)	2.2707(14)
Mo(1)–$C_{(average)}$	2.305		
$Cent_{(Tol)}$–Mo(1)–P(1)	130.38	P(1)–Mo(1)–P(1*)	99.23(2)
$Cent_{(Tol)}$–Mo(1)–O(1)	108.44	O(1)–Mo(1)–O(1*)	143.11(5)
P(1)–Mo(1)–O(1)	76.23(3)	P(1)–Mo(1)–O(1*)	80.09(3)

Similar four-legged piano stool structures with *trans* phosphine ligands have been observed for 17-electron complexes of the form [$MoCpX_2L_2$] [L_2 = bis(diphenylphosphino)ethane (dppe) and X = Cl [32] or OH [33]] and for the molybdenum (II) complexes [$MoMe_2(\eta^6$-$C_6H_5R)(PPhMe_2)_2$] (R = H, Me).[23]

There is also a considerable distortion from planarity of the η^6-arene ligands. For the benzene complex **3a**, the arene ligand adopts an inverted boat conformation with 2 carbon atoms pushed away from the Mo centre, resulting in a fold angle (θ) of approximately 13° at the C(21)–C(21*) vector. This distortion is consistent with previously observed Mo-arene complexes and a justification based on molecular orbital considerations has been proposed.[27] The distortion also results in a disruption of the π delocalisation within the arene. This is reflected in the C–C bond lengths, with 2 slightly lengthened bonds (1.434 Å) and 4 shorter bonds (average 1.40 Å).

Table 4 Selected bond lengths (Å) and angles (°) for **3b**

Mo(1)–P(2)	2.4548(6)	Mo(1)–C(46)	2.264(2)
Mo(1)–P(24)	2.4450(5)	Mo(1)–C(47)	2.372(2)
Mo(1)–O(17)	2.1182(13)	Mo(1)–C(48)	2.321(2)
Mo(1)–O(33)	2.1163(13)	Mo(1)–C(49)	2.269(2)
		Mo(1)–C(50)	2.370(2)
		Mo(1)–C(51)	2.306(2)
		Mo(1)–$Cent_{(Tol)}$	1.838
		Mo(1)–$C_{(average)}$	2.315
$Cent_{(Tol)}$–Mo(1)–P(2)	131.35	P(2)–Mo(1)–P(24)	98.62(2)
$Cent_{(Tol)}$–Mo(1)–P(24)	130.05	P(2)–Mo(1)–O(17)	76.26(4)
$Cent_{(Tol)}$–Mo(1)–O(17)	108.22	P(2)–Mo(1)–O(33)	80.11(4)
$Cent_{(Tol)}$–Mo(1)–O(33)	108.10	P(24)–Mo(1)–O(17)	80.47(4)
O(17)–Mo(1)–O(33)	143.71(5)	P(24)–Mo(1)–O(33)	76.27(4)

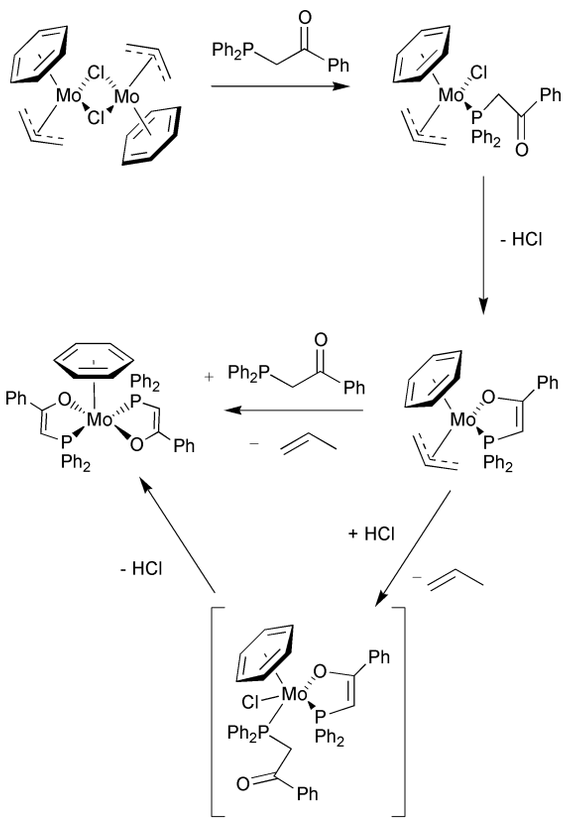

Scheme 2

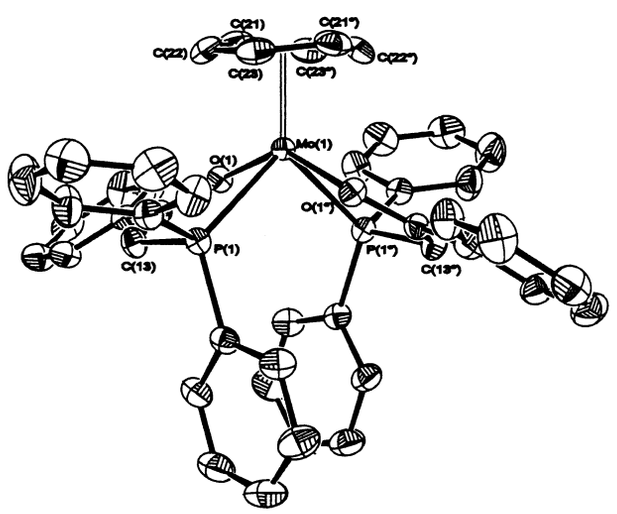

Fig. 3 The molecular structure of [Mo{$Ph_2PCH\cdots C(\cdots O)Ph$-$\kappa^2$-*P,O*}$_2$($\eta^6$-$C_6H_6$)], **3a** (50% thermal ellipsoids). Hydrogen atoms and phenyl ring carbon atom labels have been omitted for clarity.

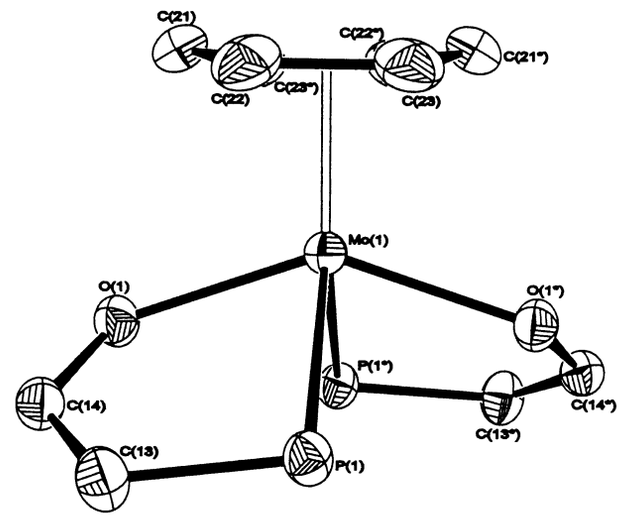

Fig. 4 Partial molecular structure of [Mo{$Ph_2PCH\cdots C(\cdots O)Ph$-$\kappa^2$-*P,O*}$_2$($\eta^6$-$C_6H_6$)], **3a** (50% thermal ellipsoids), showing coordination about the metal centre.

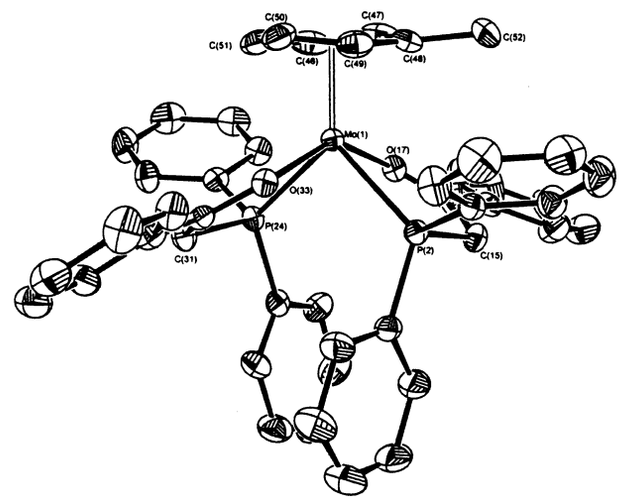

Fig. 5 The molecular structure of [Mo{$Ph_2PCH\cdots C(\cdots O)Ph$-$\kappa^2$-*P,O*}$_2$($\eta^6$-$C_6H_5Me$)], **3b** (50% thermal ellipsoids). Hydrogen atoms and phenyl ring carbon atom labels have been omitted for clarity.

However, substitution of the η^6-benzene for an η^6-toluene ligand results in a twist–boat distortion of the arene, with two carbon atoms pulled closer to the metal, two at an intermediate distance and two pushed further away. A distortion of this type has been observed for a tantalum arene complex and arguments based on molecular orbital calculations are proposed to explain the unusual distortion.[28]

The structural features of the η^1-ketophosphine and η^2-phosphinoenolate ligands in complexes **1** and **3**, in addition to the η^2-amidophosphine ligand in complex **6**·CH_2Cl_2, are presented in Table 6. The coordination mode of the heterodifunctional ligand has little effect upon the structural features of the η^6-arene or η^3-allyl ligands. Similarly, substitution of the η^6-arene ligand has no effect upon the bond lengths and angles of the η^2-phosphinoenolate fragment (compare **3a** and **3b**).

However, deprotonation of the η^1-ketophosphine ligand to form the bidentate phosphinoenolate results in a shortening of the Mo–P, P–C and C–C bonds, while a lengthening of the C–O bond is observed. This is consistent with an increase in the P–C and C–C bond orders due to a change in hybridisation of the methylene carbon. The lengthening of the C–O bond is due to a reduction in the bond order from a double bond to more single bond character.

The structural features observed in the current work are consistent with those observed for the corresponding Group

Table 5 Selected bond lengths (Å) and angles (°) for **6**·CH_2Cl_2

Mo(1)–C(27)	2.248(3)	Mo(1)–C(30)	2.295(3)
Mo(1)–C(28)	2.201(3)	Mo(1)–C(31)	2.276(3)
Mo(1)–C(29)	2.263(3)	Mo(1)–C(32)	2.366(3)
$Mo(1)–Cent_{(allyl)}$	1.978	Mo(1)–C(33)	2.304(3)
$Mo(1)–C_{(average)}$	2.24	Mo(1)–C(34)	2.253(3)
		Mo(1)–C(35)	2.388(3)
Mo(1)–P(1)	2.4603(7)	$Mo(1)–Cent_{(Tol)}$	1.833
Mo(1)–O(1)	2.220(2)	$Mo(1)–C_{(average)}$	2.31
$Cent_{(Tol)}–Mo(1)–Cent_{(allyl)}$	130.8	$Cent_{(allyl)}–Mo(1)–O(1)$	96.8
$Cent_{(Tol)}–Mo(1)–O(1)$	120.7	$Cent_{(allyl)}–Mo(1)–P(1)$	94.4
$Cent_{(Tol)}–Mo(1)–P(1)$	123.4	O(1)–Mo(1)–P(1)	75.07(6)

Table 6 Structural features of arene–molybdenum complexes containing heterodifunctional P,O donor ligands

	1b	**3b**		**3a**	**6**·CH_2Cl_2
$Mo–Ct_{(Tol)}$/Å	1.84	1.84		1.83	1.83
$Mo–C_{(Tol\text{-}average)}$/Å	2.31	2.32		2.31	2.31
$Mo–Ct_{(allyl)}$/Å	1.98	—	—	—	1.98
$Mo–C_{(allyl\text{-}average)}$/Å	2.23	—	—	—	2.24
Mo–P/Å	2.53	2.45	2.46	2.44	2.46
Mo–O/Å	—	2.12	2.12	2.11	2.22
P–C/Å	1.85	1.77	1.78	1.77	1.85
C–C/Å	1.50	1.36	1.36	1.36	1.50
C–O/Å	1.22	1.32	1.32	1.32	1.25
P–C–C/°	113.5	113.9	113.3	113.4	106.7
C–C–O/°	121.8	123.0	123.0	122.7	120.1
P–Mo–O/Cl/°	79.7	76.3	76.3	76.2	75.1

10 complexes.[34–37] However, a slight variation in the bite angle of the phosphinoenolate ligand is observed between the square planar Group 10 complexes (P–M–O = 82–87°) and the Mo(II) d^4 complexes (P–Mo–O = 75–76.3°). The PCCO bite angles observed for the phosphinoenolate complexes are similar to the bite angles of 74.76(4) and 74.37(9)° observed in [$MoCpCl_3\{Ph_2PCH_2C(O)NPh_2$-$\kappa^2P,O\}$] [74.76(4)°] and [$MoCp^*Cl_3\{Ph_2PCH_2C(O)NPh_2$-$\kappa^2P,O\}$][$BF_4$], respectively.[15]

Preparation of η^2-ketophosphine complexes

Although the β-ketophosphine ligand $Ph_2PCH_2C(O)Ph$ readily coordinates with the Mo(η^3-allyl)(η^6-arene) centre as a simple monodentate phosphine and as a bidentate phosphinoenolate, attempts to prepare cationic η^2-ketophosphine complexes *via* chloride abstraction from the phosphine-chloride complex **1** proved unsuccessful. However, treatment of the phosphinoenolate complexes [Mo(η^3-C_3H_5){$Ph_2PCH\cdots C(\cdots O)Ph$-$\kappa^2P,O$}($\eta^6$-$C_6H_5R$)], **2**, with pyridinium hexafluorophosphate resulted in protonation of the enolate ligand to give [Mo(η^3-C_3H_5){$Ph_2PCH_2C(O)Ph$-κ^2P,O}(η^6-C_6H_5R)][PF_6] [R = H (**4a**), Me (**4b**)] as deep purple solids in 70–90% yield (Scheme 1).

The ^{31}P NMR spectra exhibited resonances shifted approximately 34 ppm downfield of the chemical shifts for the corresponding phosphine-chloride complexes **1** (Table 1). This is consistent with the coordination of the phosphorus atom to a cationic molybdenum(II) centre.[15]

Hydrogen–deuterium exchange in η^2-ketophosphine and η^2-phosphinoenolate complexes

Treatment of a CD_2Cl_2 solution of **4** with an excess of D_2O resulted in the methylene protons of the chelating ketophosphine ligand undergoing hydrogen–deuterium exchange (Scheme 1). The hydrogen–deuterium exchange of the methylene protons was also observed in methanol-d_4.

To date, no similar hydrogen–deuterium exchange of methylene hydrogens with D_2O has been observed. An acid catalysed exchange has been observed in cobalt malonato complexes in the presence of D_2SO_4/D_2O.[38] However, in this case, the exchange was proposed to proceed *via* initial protonation of a carbonyl group followed by a keto–enol type tautomerisation. A similar mechanism has also been proposed for isotopic exchange observed, under acidic conditions, in polyamine-carboxylic acids complexed to cobalt.[39–41]

Treatment of a CD_2Cl_2 solution of **4a** with a large excess of pyridinium-*d* hexafluorophosphate at room temperature did not result in any hydrogen–deuterium exchange after 30 min. However, after heating at 50 °C for 10 min and standing overnight, the ^1H NMR spectrum indicated that 95% of the methylene hydrogens of the ketophosphine ligand had been exchanged for deuterium. The observation of very little exchange prior to heating probably results from the poor solubility of the pyridinium salt in dichloromethane.

In order to try and probe the mechanism of the H–D exchange, the monodeuterated complex **4a**-*d* was prepared.

The phosphinoenolate complex **2a** was treated with one equivalent of deuteropyridinium hexafluorophosphate (prepared by stirring pyridinium hexafluorophosphate in D_2O, removal of all solvent and recrystallisation from methanol-*d*) to yield the monodeutero complex [Mo(η^3-C_3H_5){$Ph_2PC(H)$-$DC(O)Ph$-κ^2P,O}(η^6-C_6H_6)][PF_6] **4a**-*d*.

The ^1H NMR spectrum of **4a**-*d* exhibited 2 broad peaks corresponding to the methylene protons of the ketophosphine ligand. Each resonance integrated as half a proton, indicating an equal distribution of deuterium at each position. Furthermore, the 2D ^1H–^1H COSY NMR experiment showed no cross peak between the two methylene resonances, indicating that $Ph_2PC(H)(D)C(Ph)O$ was the major species present in solution. No cross peaks attributed to the bis-protio species were observed. However, a statistical distribution of products would result in only 25% of the sample consisting of this species. The distribution observed is consistent with the mechanism proposed in Scheme 3.

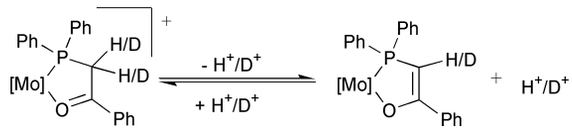

Scheme 3

Treatment of a CD_2Cl_2 or C_6D_6 solution of **2a** with D_2O resulted in the olefinic hydrogen of the phosphinoenolate ligand undergoing hydrogen–deuterium exchange. Similarly, treatment of a CD_2Cl_2 solution of the bis-phosphinoenolate complex **3a** with D_2O also resulted in the olefinic hydrogens of the enolate ligands undergoing hydrogen–deuterium exchange.

The observed exchange can be accounted for by formal protonation of the phosphinoenolate ligand by D^+ and deprotonation by OD^- to give the deuterated complex and HOD. Attack by D^+ could occur directly at the olefinic carbon of the enolate ligand or at the oxygen atom.

Similar exchange reactions were attempted with the free ligand, $Ph_2PCH_2C(O)Ph$, and with the η^1-phosphine complexes **1**. No comparable exchange was observed in either case. Therefore, it can be concluded that chelation of the P,O fragment to

the metal centre enhances the acidic character of the hydrogens in the α-CO position.

All observations of exchange between hydrogen and deuterium in methylene and olefinic groups are consistent with a dissociative mechanism explained by a simple equilibrium between protonated and deprotonated forms of the complex (Scheme 3).

Reactions of $[Mo(\eta^3\text{-}C_3H_5)(\mu\text{-}Cl)(\eta^6\text{-}C_6H_5Me)]_2$ with $Ph_2PCH_2C(O)NPh_2$

The reaction between $[Mo(\eta^3\text{-}C_3H_5)(\mu\text{-}Cl)(\eta^6\text{-}C_6H_5Me)]_2$ and the amidophosphine $Ph_2PCH_2C(O)NPh_2$ in ethanol, in the presence of excess ammonium chloride, resulted in cleavage of the chloride bridge to form the phosphine adduct $[Mo(\eta^3\text{-}C_3H_5)Cl\{Ph_2PCH_2C(O)NPh_2\text{-}\kappa^2P,O\}(\eta^6\text{-}C_6H_5Me)]$, **5**, as a red–purple solid in 63% yield (Scheme 4). In non-polar solvents, the amidophosphine behaves as a monodentate phosphorus ligand, as in the ketophosphine complexes **1**. The ^{31}P NMR chemical shift of δ 40.0 ppm (in CD_2Cl_2) is consistent with coordination of the phosphorus to a molybdenum(II) metal centre.[15] The IR spectrum confirmed that the carbonyl fragment is not coordinated to the metal centre (ν_{CO} 1668 *vs.* 1658 cm^{-1} for the free ligand[30]).

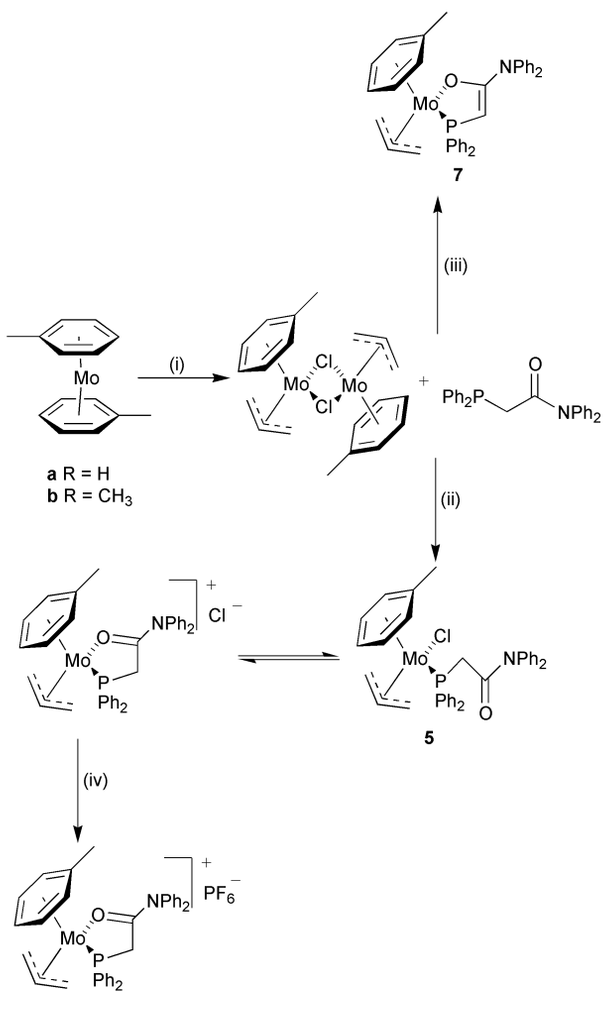

Scheme 4 *Reagents and conditions*: (i) C_3H_5Cl; (ii) ethanol, NH_4Cl; (iii) ethanol, NEt_3; (iv) ethanol, KPF_6.

However, the ^{31}P NMR spectrum recorded in acetone-d_6 exhibited 2 singlets at δ 60.1 and 39.2 ppm, in a ratio of approximately one to one. The observed chemical shifts are consistent with the existence of an equilibrium between the neutral phosphine complex **5** and the cationic complex $[Mo(\eta^3\text{-}C_3H_5)\{Ph_2PCH_2C(O)NPh_2\text{-}\kappa^2P,O\}(\eta^6\text{-}C_6H_5Me)][Cl]$, in which the carbonyl functionality has displaced the chloride ligand (Scheme 4). In benzene-d_6, a ratio of approximately 95% neutral species and 5% cationic species was observed in the ^{31}P NMR spectrum.

The cationic complex $[Mo(\eta^3\text{-}C_3H_5)\{Ph_2PCH_2C(O)NPh_2\text{-}\kappa^2P,O\}(\eta^6\text{-}C_6H_5Me)][PF_6]$, **6**, was isolated from the reaction of **5** with potassium hexafluorophosphate in hot ethanol (Scheme 4). Compound **6** was obtained as a red–purple solid in 73% yield. Coordination of the carbonyl fragment to the molybdenum(II) centre was confirmed by the IR spectrum, which displayed a peak at 1554 cm^{-1} (*versus* 1658 cm^{-1} for the free ligand).

X-Ray quality crystals of **6**·CH_2Cl_2 were grown *via* the slow diffusion of pentane into a concentrated dichloromethane solution of the complex. The molecular structure of the cation **6** is shown in Fig. 6. Selected bond distances and angles are presented in Table 5.

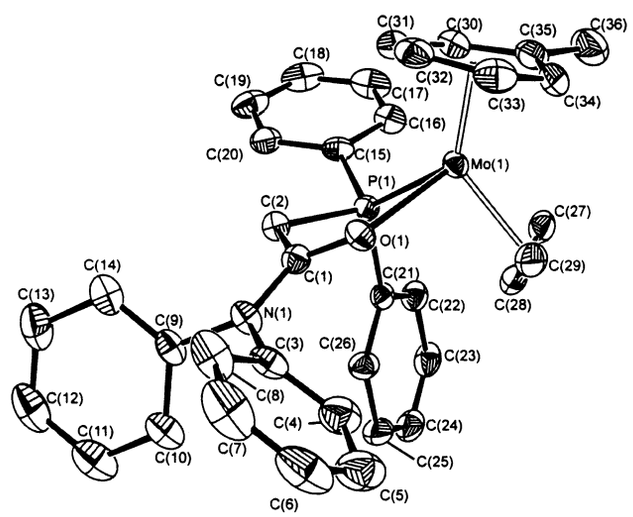

Fig. 6 The molecular structure of the cation in $[Mo(\eta^3\text{-}C_3H_5)\{Ph_2PCH_2C(O)NPh_2\text{-}\kappa^2P,O\}(\eta^6\text{-}C_6H_5Me)][PF_6]\cdot CH_2Cl_2$, **6**·$CH_2Cl_2$ (50% thermal ellipsoids). Hydrogen atoms, the counterion and the dichloromethane molecule have been omitted for clarity.

Complex **6** crystallised with one equivalent of dichloromethane contained in the crystal lattice. As observed in the other crystal structures described here, the cation of complex **6** adopts a three-legged piano stool type structure. The structural features of the amidophosphine fragment (Table 6) are consistent with those observed in $[MoCpCl_3\{Ph_2PCH_2C(O)NPh_2\text{-}\kappa^2P,O\}]$ and $[MoCp^*Cl_3\{Ph_2PCH_2C(O)NPh_2\text{-}\kappa^2P,O\}][BF_4]$.[15]

The reaction between $[Mo(\eta^3\text{-}C_3H_5)(\mu\text{-}Cl)(\eta^6\text{-}C_6H_5Me)]_2$ and $Ph_2PCH_2C(O)NPh_2$ in the presence of excess triethylamine and ethanol as solvent yielded the η^2-phosphinoenolate complex $[Mo(\eta^3\text{-}C_3H_5)\{Ph_2PCHC(O)NPh_2\text{-}\kappa^2P,O\}(\eta^6\text{-}C_6H_5Me)]$, **7**, as an orange solid in 63% yield (Scheme 4).

Investigations into the reaction between $[Mo(\eta^3\text{-}C_3H_5)(\mu\text{-}Cl)(\eta^6\text{-}C_6H_5Me)]_2$ and $Ph_2PCH_2C(O)NPh_2$ in ethanol, indicated that a mixture of products was formed. The η^2-phosphinoenolate complex **7** was isolated from the reaction in 22% yield, while ^{31}P NMR analysis of the residue indicated the product to be an equilibrium between **5** and the cationic complex $[Mo(\eta^3\text{-}C_3H_5)\{Ph_2PCH_2C(O)NPh_2\text{-}\kappa^2P,O\}(\eta^6\text{-}C_6H_5Me)]Cl$.

Conclusion

The reactions of the P,O ligands $Ph_2PCH_2C(O)R$ (R = Ph, NPh_2) with the η^6-arene molybdenum complexes $[Mo(\eta^3\text{-}C_3H_5)(\mu\text{-}Cl)(\eta^6\text{-}C_6H_5R)]_2$ (R = H, Me) have been investigated. The ketophosphine ligand $Ph_2PCH_2C(O)Ph$ reacted with the molybdenum centres to form complexes in which the P,O ligand displayed η^1-phosphine, $[Mo(\eta^3\text{-}C_3H_5)Cl(\eta^6\text{-}C_6H_5R)\{Ph_2PCH_2C(O)Ph\}]$, and η^2-phosphinoenolate coordination,

$[Mo(\eta^3\text{-}C_3H_5)\{Ph_2PCH\cdots C(\cdots O)Ph\text{-}\kappa^2P,O\}(\eta^6\text{-}C_6H_5R)]$. An interesting bis-$\eta^2$-phosphinoenolate complex, $[Mo\{Ph_2PCH\cdots C(\cdots O)Ph\text{-}\kappa^2P,O\}_2(\eta^6\text{-}C_6H_5R)]$, which combines a classic co-ordination chemistry core with a non-classical η^6-arene ligand was also prepared and structurally characterised. The corresponding cationic η^2-ketophosphine complexes, $[Mo(\eta^3\text{-}C_3H_5)\{Ph_2PCH_2C(O)Ph\text{-}\kappa^2P,O\}(\eta^6\text{-}C_6H_5R)][PF_6]$, were prepared from the protonation of η^2-phosphinoenolate complexes. An unprecedented hydrogen–deuterium exchange of methylene and olefinic hydrogens with D_2O was observed.

The amidophosphine ligand $Ph_2PCH_2C(O)NPh_2$ displayed similar reactivity to form η^1-phosphine, $[Mo(\eta^3\text{-}C_3H_5)Cl(\eta^6\text{-}C_6H_5Me)\{Ph_2PCH_2C(O)NPh_2\}]$, and η^2-phosphinoenolate, $[Mo(\eta^3\text{-}C_3H_5)(\eta^6\text{-}C_6H_5Me)\{Ph_2PCH\cdots C(\cdots O)NPh_2\text{-}\kappa^2P,O\}]$, complexes. However, in contrast to $Ph_2PCH_2C(O)Ph$, in polar solvents such as acetone, the η^1-phosphine chloride complex displayed more typical hemilabile ligand characteristics and an equilibrium with the cationic η^2-amidophosphine complex $[Mo(\eta^3\text{-}C_3H_5)\{Ph_2PCH_2C(O)NPh_2\text{-}\kappa^2P,O\}(\eta^6\text{-}C_6H_5Me)]Cl$ was observed. This allowed the latter complex to be isolated *via* anion metathesis with potassium hexafluorophosphate.

The crystal structures of the compounds $[Mo(\eta^3\text{-}C_3H_5)Cl(\eta^6\text{-}C_6H_5Me)\{Ph_2PCH_2C(O)Ph\}]$, $[Mo(\eta^3\text{-}C_3H_5)\{Ph_2PCH_2C(O)NPh_2\text{-}\kappa^2P,O\}(\eta^6\text{-}C_6H_5Me)][PF_6]$ and $[Mo\{Ph_2PCH\cdots C(\cdots O)Ph\text{-}\kappa^2P,O\}_2(\eta^6\text{-}C_6H_5R)]$ (R = H, Me) have been determined.

Experimental

General

All manipulations of air and/or moisture sensitive materials were performed under an inert atmosphere of argon using standard Schlenk line techniques, or in an inert atmosphere dry box containing dinitrogen. Solvents were dried over the appropriate drying agent and distilled under nitrogen. Deuterated solvents were dried over the appropriate drying agent and vacuum distilled prior to use. The compounds $[Mo(\eta^3\text{-}C_3H_5)(\mu\text{-}Cl)(\eta^6\text{-}C_6H_5R)]_2$ (R = H, Me),[42] $Ph_2PCH_2C(O)Ph$[20] and $Ph_2PCH_2C(O)NPh_2$[43] were prepared according to previously published methods. Triethylamine was purchased from the Aldrich Chemical Company, dried over calcium hydride and distilled under nitrogen prior to use. Pyridinium hexafluorophosphate was prepared *via* the protonation of pyridine with excess hexafluorophosphoric acid (60% solution in water) in diethyl ether, followed by recrystallisation from ethanol.

NMR spectra were recorded on Varian Mercury 300 (^{1}H, ^{13}C, ^{19}F and ^{31}P at 300.17, 75.48, 282.40 and 121.51 MHz, respectively) or Varian UnityPlus 500 (^{1}H at 499.99 MHz) spectrometers at room temperature in benzene-d_6 or dichloromethane-d_2. They were referenced internally using the residual protio solvent (^{1}H) and solvent (^{13}C) resonances and measured relative to tetramethylsilane (^{1}H and ^{13}C; δ 0 ppm). ^{31}P and ^{19}F NMR were referenced externally to 85% H_3PO_4 (δ 0 ppm) and $CFCl_3$ (δ 0 ppm), respectively. Elemental analyses were provided by the microanalytical department, Inorganic Chemistry Laboratory, University of Oxford. Infra-red spectra were recorded from Nujol mulls on a Perkin Elmer 1600 Series FTIR spectrometer.

Preparations

$[Mo(\eta^3\text{-}C_3H_5)Cl(\eta^6\text{-}C_6H_6)\{Ph_2PCH_2C(O)Ph\}]$, 1a. The complex $[Mo(\eta^3\text{-}C_3H_5)(\mu\text{-}Cl)(\eta^6\text{-}C_6H_6)]_2$ (200 mg, 0.4 mmol) and $Ph_2PCH_2C(O)Ph$ (250 mg, 0.82 mmol) were combined as solids and suspended in ethanol (20 ml). The reaction mxture was stirred at 45 °C for 4 h and at room temperature for a further 12 h. The resulting purple precipitate was isolated by filtration and recrystallised from dichloromethane–pentane. Complex **1a** (290 mg, 0.52 mmol, 65%) was obtained as a purple crystalline solid.

$[Mo(\eta^3\text{-}C_3H_5)Cl(\eta^6\text{-}C_6H_5Me)\{Ph_2PCH_2C(O)Ph\}]$, 1b. This compound was prepared in a similar manner to **1a**, starting from $[Mo(\eta^3\text{-}C_3H_5)(\mu\text{-}Cl)(\eta^6\text{-}C_6H_5Me)]_2$ (300 mg, 0.57 mmol) and $Ph_2PCH_2C(O)Ph$ (710 mg, 2.34 mmol). However, the reaction was carried out at room temperature for 15 h. Complex **1b** (390 mg, 0.69 mmol, 61%) was obtained as a purple–red crystalline solid.

$[Mo(\eta^3\text{-}C_3H_5)\{Ph_2PCH\cdots C(\cdots O)Ph\text{-}\kappa^2P,O\}(\eta^6\text{-}C_6H_6)]$, 2a. The complex $[Mo(\eta^3\text{-}C_3H_5)(\mu\text{-}Cl)(\eta^6\text{-}C_6H_6)]_2$ (500 mg, 1 mmol) and $Ph_2PCH_2C(O)Ph$ (700 mg, 2.3 mmol) were combined as solids and suspended in ethanol (30 ml). Excess triethylamine (3 ml) was added and the reaction mixture stirred at 50 °C for 4 h. After stirring at room temperature overnight, the resulting red–orange precipitate was isolated by filtration, washed with pentane and dried *in vacuo*. The crude product was recrystallised from dichloromethane–pentane. Complex **2a** (850 mg, 1.64 mmol, 82%) was obtained as an orange–red crystalline solid.

$[Mo(\eta^3\text{-}C_3H_5)\{Ph_2PCH\cdots C(\cdots O)Ph\text{-}\kappa^2P,O\}(\eta^6\text{-}C_6H_5Me)]$, 2b. This compound was prepared in a similar manner to **2a**, starting from $[Mo(\eta^3\text{-}C_3H_5)(\mu\text{-}Cl)(\eta^6\text{-}C_6H_5Me)]_2$ (600 mg, 1.13 mmol) and $Ph_2PCH_2C(O)Ph$ (730 mg, 2.4 mmol). However, the reaction was carried out at room temperature. Complex **2b** (820 mg, 1.5 mmol, 66%) was obtained as an orange crystalline solid.

$[Mo\{Ph_2PCH\cdots C(\cdots O)Ph\text{-}\kappa^2P,O\}_2(\eta^6\text{-}C_6H_6)]$, 3a. The complex $[Mo(\eta^3\text{-}C_3H_5)(\mu\text{-}Cl)(\eta^6\text{-}C_6H_6)]_2$ (300 mg, 0.60 mmol) and $Ph_2PCH_2C(O)Ph$ (750 mg, 2.47 mmol) were combined as solids and suspended in ethanol (30 ml). The reaction mixture was heated at reflux for 3 h. After cooling to room temperature, the solution was filtered to yield a small amount of red–brown solid. The precipitate was dried *in vacuo* and recrystallised from dichloromethane–pentane. Complex **3a** (180 mg, 0.23 mmol, 19%) was obtained as a red crystalline solid.

$[Mo\{Ph_2PCH\cdots C(\cdots O)Ph\text{-}\kappa^2P,O\}_2(\eta^6\text{-}C_6H_5Me)]$, 3b. The complex $[Mo(\eta^3\text{-}C_3H_5)(\mu\text{-}Cl)(\eta^6\text{-}C_6H_5Me)]_2$ (300 mg, 0.57 mmol) and $Ph_2PCH_2C(O)Ph$ (400 mg, 1.32 mmol) were combined as solids and suspended in ethanol (30 ml). The reaction mixture was heated at 85 °C for 1.5 h and then stirred at room temperature for 12 h. The solution was filtered to yield a dark coloured precipitate. The crude product was recrystallised from dichloromethane–pentane. Complex **3b** (120 mg, 0.15 mmol, 13%) was obtained as a deep red crystalline solid.

$[Mo(\eta^3\text{-}C_3H_5)\{Ph_2PCH_2C(O)Ph\text{-}\kappa^2P,O\}(\eta^6\text{-}C_6H_6)][PF_6]$, 4a. The phosphinoenolate complex **2a** (100 mg, 0.19 mmol) and pyridinium hexafluorophosphate (43 mg, 0.19 mmol) were combined as solids and ethanol (15 ml) added. A deep purple colour rapidly formed and the reaction was stirred at room temperature for 15 h. The resulting purple precipitate was isolated by filtration, washed with toluene (5 ml) and pentane and dried *in vacuo*. Complex **4a** (110 mg, 0.17 mmol, 87%) was obtained as a purple crystalline solid.

$[Mo(\eta^3\text{-}C_3H_5)\{Ph_2PCH_2C(O)Ph\text{-}\kappa^2P,O\}(\eta^6\text{-}C_6H_5Me)][PF_6]$, 4b. This compound was prepared in a similar manner to **4a**, starting from **2b** (150 mg, 0.28 mmol) and pyridinium hexafluorophosphate (70 mg, 0.31 mmol). Complex **4b** (160 mg, 0.21 mmol, 75%) was obtained as a purple crystalline solid, with one equivalent of dichloromethane in the crystal lattice.

Pyridinium-*d* hexafluorophosphate. Pyridinium hexafluorophosphate was dissolved in excess D_2O and stirred at room temperature for 30 min. The solvent was removed *in vacuo* and the residue recrystallised from methanol-*d* (MeOD) at −78 °C.

Table 7 Crystal data and structure refinement for compounds **1b**, **3a**, **3b** and **6**·CH_2Cl_2

	1b	**3a**	**3b**	**6**
Empirical formula	$C_{30}H_{30}ClMoOP$	$C_{23}H_{19}Mo_{0.5}OP$	$C_{47}H_{39}MoO_2P_2$	$C_{36.5}H_{37}ClF_6MoNOP_2$
Formula weight	568.93	390.35	793.71	813.03
Crystal system	Monoclinic	Monoclinic	Monoclinic	Monoclinic
Space group	*C*2/*c*	*C*2/*c*	$P2_1/n$	$P2_1/n$
a/Å	25.516(2)	12.0880(3)	12.5120(3)	11.0924(2)
b/Å	9.196(4)	14.8310(4)	14.7700(3)	21.8354(4)
c/Å	23.678(2)	20.3990(5)	20.2580(3)	14.7699(3)
β/°	112.973(2)	95.400(2)	95.413(1)	102.7274(8)
U/Å^3	5115.3	3640.8	3727.0	3489.5
Z	8	8	4	4
T/K	150	190	190	150
μ/mm^{-1}	0.701	0.488	0.478	0.608
Reflections collected	20774	10555	29614	14831
Independent reflections	4959	3708	7628	7947
R	0.0586	0.0262	0.0438	0.0432
R_w	0.0374	0.0309	0.0320	0.0516

[Mo(η^3-C_3H_5)Cl(η^6-C_6H_5Me){$Ph_2PCH_2C(O)NPh_2$}], 5. The complex [Mo(η^3-C_3H_5)(μ-Cl)(η^6-C_6H_5Me)]$_2$ (200 mg, 0.38 mmol), $Ph_2PCH_2C(O)NPh_2$ (310 mg, 0.78 mmol) and ammonium chloride (220 mg, 4.1 mmol) were combined as solids and suspended in ethanol (30 ml). The reaction mixture was stirred at 60 °C for 1 h, then at room temperature for 15 h. The resulting red–purple precipitate was isolated by filtration and recrystallised from toluene. Complex **5** (320 mg, 0.48 mmol, 63%) was obtained as a purple–red solid.

[Mo(η^3-C_3H_5){$Ph_2PCH_2C(O)NPh_2$-κ^2*P,O*}(η^6-C_6H_5Me)][PF_6], 6. Complex **5** (100 mg, 0.15 mmol) was dissolved in boiling ethanol (15 ml) and excess potassium hexafluorophosphate added. The reaction mixture was allowed to cool to room temperature and stirred for 4 h. The resulting red–purple precipitate was isolated by filtration and recrystallised from dichloromethane–pentane. Complex **6** (85 mg, 0.11 mmol, 73%) was obtained as a purple–red crystalline solid.

[Mo(η^3-C_3H_5){$Ph_2PCH{\cdots}C({\cdots}O)NPh_2$-κ^2*P,O*}(η^6-$C_6H_5Me$)], 7. The complex [Mo(η^3-C_3H_5)(μ-Cl)(η^6-C_6H_5Me)]$_2$ (200 mg, 0.38 mmol) and $Ph_2PCH_2C(O)NPh_2$ (310 mg, 0.78 mmol) were combined as solids and suspended in ethanol (20 ml). Excess triethylamine (2 ml) was added and the reaction stirred at room temperature for 24 h. The resulting orange precipitate was isolated by filtration and recrystallised from dichloromethane–pentane. Complex **7** (300 mg, 0.48 mmol, 63%) was obtained as an orange solid.

Crystallography

Data were collected on an Enraf-Nonius DIP2000 image plate diffractometer with Mo-Kα radiation (λ = 0.71069 Å) as summarised in Table 7. For complex **6**, data were collected on a Nonius KappaCCD diffractometer with Mo-Kα radiation (λ = 0.71069 Å).

The images were processed with the DENZO[44] and SCALEPACK[45] programs. Corrections for Lorentz and polarisation effects were performed. All solution, refinement and graphical calculations were performed using the CRYSTALS,[46] SHELXL[47] and CAMERON[48] software packages.

In each case, a single crystal was encased in perfluoropolyether oil and mounted atop a glass fibre. The fibre, secured in a goniometer head, was then placed under a stream of cold nitrogen maintained at 150 K and data collected.

The structures were solved using the program SIR92[49] and refined using full-matrix least-squares on all *F* data (CRYSTALS). All non-hydrogen atoms were refined anisotropically and hydrogen atoms were included in calculated positions with isotropic thermal parameters. All calculations were carried out on a Pentium personal computer.

A Chebychev polynomial weighting scheme[50] with parameters 1.99, −0.223, 1.62 and 0.0812 was applied to complex **1b**. The structure was refined to a final *R* factor of 0.0586 and R_w = 0.0374 with a maximum residual electron density of 0.72 e Å^{-3}. Similar weighting schemes were applied to the structures of **3a** (parameters 2.46, 0.452 and 2.00; final *R* factor 0.0262; R_w = 0.0309; maximum residual electron density 0.50 e Å^{-3}), **3b** (parameters 0.319, −1.94, −0.195 and −0.765; final *R* factor 0.0438; R_w = 0.0320; maximum residual electron density 0.68 e Å^{-3}) and **6** (parameters 0.966, 0.447 and 0.689; final *R* factor 0.0432; R_w = 0.0516; maximum residual electron density 1.10 e Å^{-3}).

The crystallographic data are summarised in Table 7.

CCDC reference numbers 168488 and 168490–168492.

See http://www.rsc.org/suppdata/dt/b2/b202441c/ for crystallographic data in CIF or other electronic format.

Acknowledgements

We would like to thank The Kings School, Sydney, The University of Sydney, Australia (N. G. J.), the AG Leventis Foundation (I. V.) the EPSRC (L. H. R.), the CNRS, the Ministère de la Recherche (Paris) and the CNRS/RS cooperation programme (X. M., N. G. J.) for the provision of financial support, and the RSC for a travel grant (X. M.; JGA no. 0103306).

References

1 S. E. Bouaoud, P. Braunstein, D. Grandjean, D. Matt and D. Nobel, *Inorg. Chem.*, 1986, **25**, 3765.
2 P. Crochet, B. Demerseman, C. Rocaboy and D. Schleyer, *Organometallics*, 1996, **15**, 3048.
3 P. Crochet, B. Demerseman, M. I. Vallejo, M. P. Gamasa, J. Gimeno, J. Borge and S. Garcia-Granda, *Organometallics*, 1997, **16**, 5406.
4 P. Braunstein, Y. Chauvin, J. Nähring, A. DeCian and J. Fischer, *J. Chem. Soc., Dalton Trans.*, 1995, 863.
5 P. Braunstein, Y. Chauvin, J. Nähring, Y. Dusausoy, D. Bayeul, A. Tiripicchio and F. Ugozzoli, *J. Chem. Soc., Dalton Trans.*, 1995, 851.
6 P. Braunstein, D. G. Kelly, A. Tiripicchio and F. Ugozzoli, *Inorg. Chem.*, 1993, **32**, 4845.
7 P. Braunstein, S. Coco Cea, A. DeCian and J. Fischer, *Inorg. Chem.*, 1992, **31**, 4203.
8 D. Matt, M. Huhn, J. Fischer, A. DeCian, W. Kläui, I. Tkatchenko and M. C. Bonnet, *J. Chem. Soc., Dalton Trans.*, 1993, 1173.
9 J. Andrieu, P. Braunstein and F. Naud, *J. Chem. Soc., Dalton Trans.*, 1996, 2903.
10 J. Andrieu, P. Braunstein, F. Naud and R. D. Adams, *J. Organomet. Chem*, 2000, **601**, 43.
11 P. Braunstein, Y. Chauvin, S. Mercier, L. Saussine, A. DeCian and J. Fischer, *J. Chem. Soc., Chem. Commun.*, 1994, 2203.
12 G. J. P. Britovsek, V. C. Gibson and D. F. Wass, *Angew. Chem., Int. Ed.*, 1999, **38**, 428.

13 S. D. Ittel, L. K. Johnson and M. Brookhart, *Chem. Rev.*, 2000, **100**, 1169.
14 W. Keim, *Angew. Chem., Int. Ed. Engl.*, 1990, **29**, 235.
15 J. M. Camus, D. Morales, J. Andrieu, P. Richard, R. Poli, P. Braunstein and F. Naud, *J. Chem. Soc., Dalton Trans.*, 2000, 2577.
16 C. D. Andrews, A. D. Burrows, J. M. Lynam, M. F. Mahon and M. T. Palmer, *New J. Chem.*, 2001, **25**, 824.
17 M. L. H. Green, J. Knight, L. C. Mitchard, G. G. Roberts and W. E. Silverthorn, *J. Chem. Soc., Chem. Commun.*, 1971, 1619.
18 M. L. H. Green, L. C. Mitchard and W. E. Silverthorn, *J. Chem. Soc., Dalton Trans.*, 1973, 1403.
19 M. Canestrari, M. L. H. Green and A. Izquierdo, *J. Chem. Soc., Dalton Trans.*, 1984, 2795.
20 D. Matt, M. Huhn and P. Braunstein, *Inorg. Synth.*, 1997, **31**, 138.
21 F. Abugideiri, J. C. Fettinger, D. W. Keogh and R. Poli, *Organometallics*, 1996, **15**, 4407.
22 M. T. Ashby, V. S. Asirvatham, A. S. Kowalski and M. A. Khan, *Organometallics*, 1999, **18**, 5004.
23 J. L. Atwood, W. E. Hunter, R. D. Rogers, E. Carmona-Guzman and G. Wilkinson, *J. Chem. Soc., Dalton Trans.*, 1979, 1519.
24 P. W. Jolly, C. Krüger, C. C. Romão and M. J. Romão, *Organometallics*, 1984, **3**, 936.
25 C. P. Mehnert, A. N. Chernega and M. L. H. Green, *J. Organomet. Chem.*, 1996, **513**, 247.
26 G. Aullon, D. Bellamy, L. Brammer, E. A. Bruton and A. G. Orpen, *Chem. Commun.*, 1998, 653.
27 L. J. Radonovich, F. J. Koch and T. A. Albright, *Inorg. Chem.*, 1980, **19**, 3373.
28 P. A. Wexler, D. E. Wigley, J. B. Koerner and T. A. Albright, *Organometallics*, 1991, **10**, 2319.
29 D. J. Arney, P. A. Wexler and D. E. Wigley, *Organometallics*, 1990, **9**, 1282.
30 J. Andrieu, P. Braunstein, A. Tiripicchio and F. Ugozzoli, *Inorg. Chem.*, 1996, **35**, 5975.
31 P. Veya, C. Floriani, A. Chiesi-Villa, C. Guastini, A. Dedieu, F. Ingold and P. Braunstein, *Organometallics*, 1993, **12**, 4359.
32 J. C. Fettinger, D. W. Keogh, B. Pleune and R. Poli, *Inorg. Chim. Acta*, 1997, **261**, 1.
33 D. Morales, B. Pleune, R. Poli and P. Richard, *J. Organomet. Chem.*, 2000, **596**, 64.
34 U. Klabunde, R. Mulhaupt, T. Herskovitz, A. H. Janowicz, J. Calabrese and S. D. Ittel, *J. Polym. Sci., Part A.*, 1987, **25**, 1989.
35 P. Braunstein, L. Douce, J. Fischer, N. C. Craig, G. Goetz-Grandmont and D. Matt, *Inorg. Chim. Acta*, 1992, **194**, 151.
36 J. Andrieu, P. Braunstein, F. Naud, R. D. Adams and R. Layland, *Bull. Soc. Chim. Fr.*, 1996, **133**, 669.
37 P. Braunstein, D. Matt, D. Nobel, F. Balegroune, S. E. Bouaoud, D. Grandjean and J. Fischer, *J. Chem. Soc., Dalton Trans.*, 1988, 353.
38 M. E. Farago and M. A. R. Smith, *J. Chem. Soc., Dalton Trans.*, 1972, 2120.
39 R. D. Gillard and D. A. Phipps, *J. Chem. Soc., Chem. Comm.*, 1970, 800.
40 J. B. Terrill and C. N. Reilley, *Inorg. Chem.*, 1966, **5**, 1988.
41 J. L. Sudmeir and G. Occupati, *Inorg. Chem.*, 1968, **7**, 2524.
42 M. L. H. Green and W. E. Silverthorn, *J. Chem. Soc., Dalton Trans.*, 1973, 301.
43 J. Andrieu, P. Braunstein and A. D. Burrows, *J. Chem. Res., Synop.*, 1993, 380.
44 Z. Otwinowski, DENZO©, Department of Molecular Biophysics and Biochemistry, Yale University, New Haven, CT, USA, 1993.
45 Z. Otwinowski, SCALEPACK©, Department of Molecular Biophysics and Biochemistry, Yale University, New Haven, CT, USA, 1993.
46 D. J. Watkin, C. K. Prout, J. R. Carruthers, and P. W. Betteridge, CRYSTALS, issue 10, Chemical Crystallography Laboratory, University of Oxford, UK, 1996.
47 G. M. Sheldrick, SHELXL93, Program for Crystal Structure Refinement, Institüt für Anorganische Chemie der Universität, Göttingen, Germany, 1993.
48 D. J. Watkin, C. K. Prout, and L. J. Pearce, CAMERON, Chemical Crystallography Laboratory, University of Oxford, UK, 1996.
49 A. Altomare, G. Cascarano, C. Giacovazzo, A. Guagliardi, M. C. Burla, G. Polidori and M. Camalli, *J. Appl. Crystallogr.*, 1994, **27**, 435.
50 R. Carruthers and D. J. Watkin, *Acta Crystallogr., Sect. A*, 1979, **35**, 698.